STEADY AND UNSTEADY COMPUTATIONS OF FLOWS CLOSE TO AIRFOIL BUFFETING: VALIDATION OF TURBULENCE MODELS

Frédéric Furlano and Eric Coustols
ONERA/DMAE – Department Models for Aerodynamics and Energetics
2 avenue Edouard Belin – F-31055 Toulouse CEDEX - FRANCE
Frederic.Furlano@onecert.fr – Eric.Coustols@onecert.fr

Sylvie Plot and Olivier Rouzaud
ONERA/DSNA – Department for Computational Fluid Dynamics and Aeroacoustics
29 avenue de la Division Leclerc, B.P. 72, F-92322 Châtillon CEDEX - FRANCE
Sylvie.Plot@onera.fr – Olivier.Rouzaud@onera.fr

ABSTRACT

This paper deals with results from on-going research at ONERA, regarding validation of turbulence models for flows close to the onset of airfoil buffeting. Two- as well as three-dimensional steady RANS computations have been applied to few test cases, turbulence closure being achieved using standard transport equation models. First attempts of unsteady Navier-Stokes computations are also evoked.

INTRODUCTION

Although airfoil wing buffeting is not a destructive phenomenon, its numerical prediction is requisite since it limits the flight envelope of an aeroplane. For transonic flows, buffeting is typically caused by shock/boundary layer interaction which can result in a more or less important separated region. The computational method has to take into account the main features of the flow, viscous and unsteady effects being the most important ones.

Thus, developing such a numerical prediction requires to evaluate the ability of turbulence models to reproduce separated turbulent flows. In former studies, this evaluation has been carried out at conditions corresponding to the onset of buffeting, for which a steady approach is still valid (Furlano et al., 1999, Furlano, 2001). A RANS solver, developed at ONERA (Vuillot et al., 1993, Couaillier 1999), has been applied to several experimental cases, for which validated data are available. New developments, based upon Dual Time Step method (Rouzaud and Plot, 2000a, Rouzaud et al., 2000b), have allowed to investigate unsteadiness of the flow and then, to go further beyond the onset of buffeting.

This paper deals mainly with recent numerical results obtained in this research field, when computing the following experimental test cases:

- a two-dimensional OALT25 airfoil, tested at a free-stream Mach number, M_∞, of 0.78 and different angles of attack, α, from 1° to 2.5°;
- a two-dimensional RA16SC1 airfoil, tested at M_∞= 0.732 and α= 3° to 4°.

According both to previous studies dealing with validation of models for separated flows and the structure of the RANS solver, the turbulence models which have been eligible for the present applications are based upon the eddy viscosity concept, through the Boussinesq assumption. Thus, closure relations deal with either one- or two-transport equation models.

For the former test cases, detailed comparisons between computations and experiments are discussed, using either three-dimensional (**3D**) steady approach or two-dimensional (**2D**) unsteady approach. Emphasis is mainly set upon aerodynamic coefficients, pressure distributions, pressure fluctuations and frequency.

NAVIER-STOKES SOLVER AND TURBULENCE MODELLING

The ONERA code (Vuillot et al., 1993, Couaillier 1999) solves the three-dimensional compressible Reynolds Averaged Navier Stokes (RANS) system of equations.

Basic numerical method

The code is a multi-domain solver for structured meshes. It uses finite-volume method with a cell-centred discretisation. For computations involving transport equations turbulence models, the system of equations of the mean field and the turbulent field are uncoupled in order to keep the modular feature of the solver.

The numerical scheme is the Jameson scheme (Jameson et al., 1981). It requires to use linear and non-linear artificial dissipation terms to ensure its stability and to capture shock waves or stagnation points. The time integration corresponds to a four-stage Runge-Kutta scheme which is second-order accurate.

Dealing with steady-state computations, several convergence acceleration techniques are available

such as local time stepping, implicit residual smoothing and multi-grid method.

Lastly, unsteady simulations are also possible if global time stepping is used. However, as the choice of the time step depends only on the criterion stability of the scheme, computations tend to be very expensive.

Dual Time Step method

To overcome this problem, the dual time step method (Jameson, 1991) has been developed in the code (Rouzaud et al., 2000a and 2000b). The method is time implicit and allows to choose the time step value only relatively to the frequencies of the phenomenon under investigation.

Having defined a fictitious time "the dual time", sub-iterations are performed at each physical time step to solve the equations. The sub-iterations process is equivalent to a steady-state process with respect to the dual time. By the way, convergence acceleration techniques previously mentioned are usable.

To limit the number of sub-iterations, a tolerance criterion has been defined for each system of equations. It is based on the L2-norm of the residual variations for the density variable and the first turbulent variable (for instance, ρk for the Jones-Launder model). For present computations, the tolerance criterion values are respectively equal to 10^{-4} and 10^{-3}.

Turbulence modelling

Turbulence closure is achieved using Boussinesq assumption. Then, the turbulent viscosity, μ_t, present in the Reynolds stress tensor, is expressed using the turbulence length and velocity scales, obtained by solving transport equations. Several one- and two-layer transport-equation models have been tested for the present applications:

- the one-layer Spalart-Allmaras [SA] model (Spalart et Allmaras, 1994);
- the one-layer two transport equations models: k-ε from Jones-Launder [JL] (Jones and Launder, 1972) and k-l from Smith [Sm] (Smith, 1994); where ε is the dissipation rate and l a length scale representative of turbulence;
- the two-layer transport-equation model k-ω/k-ε from Menter [SST], including SST corrector on the turbulent viscosity level (Menter, 1994);
- the two-layer transport equation model k-l/k-φ [KPHI] from ONERA (Cousteix et al., 1997), where $\varphi=\varepsilon/k^{(1/2)}$.

Boundary conditions

At the wall, the no-slip condition is prescribed. For the turbulent field, the boundary conditions are strongly dependent upon the turbulence model. For the far-field boundaries, non-reflecting boundary condition is applied.

2D/3D STEADY TRANSONIC STUDY: OALT25 AIRFOIL

Experimental data base

Tests were conducted in the ONERA T2 wind tunnel with the 2D OALT25 airfoil (c, chord length: 250mm, relative thickness: 12.18%). The model is equipped with 47 pressure taps in a section almost aligned with the free-stream direction. A large number of pressure taps (58) has been placed along the axis of the upper and lower adaptive walls of the test section.

Thus, pressure distributions have been obtained for different angles of attack of the model (0.5° to 2.5°); for a given free stream Mach number M_∞=0,78, measurements have been carried out for several values of stagnation pressure and temperature (including cryogenic conditions) allowing to reach chord Reynolds numbers, Rc, of 5.8 10^6 and 20.15 10^6 (Caruana et al., 1996).

2D results

At first, 2D computations have been performed. Due to a grid convergence study, we have retained a C-type mesh which contains 321*97 points. The mesh satisfies the far-field vortex condition (Thomas and Salas, 1986). Therefore, the reduced height y^+ of the cell adjacent to the wall is between 0.4 and 0.7 upstream of the shock.

Side walls effects have been taken into account by slightly rectifying the value of M_∞ and α (respectively, ΔM_∞=-0.01 and $\Delta\alpha$=-0.3°). These corrections have been estimated with an inviscid/viscous coupling method.

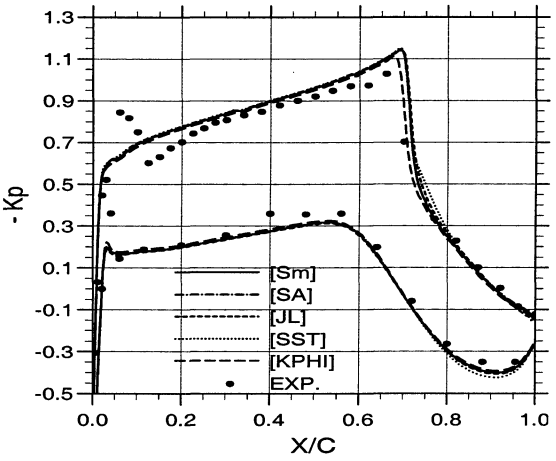

Figure 1 : OALT25 airfoil. Pressure distribution. (321*97) mesh. M_∞=0.78, α=1°, Rc=20.15 10^6.

Results obtained with five turbulence models are illustrated in Fig. 1 for an angle of attack of 1° and Rc=20.15 10^6. In the tests, transition tripping was optimised for Rc=5.8 10^6 at x/c=5% on both sides of the airfoil, which explains the recorded perturbation in the trip area, where the local Mach number is just above 1.

The results are in fair agreement between all turbulence models although slight differences are visible on the shock location and the strength of the pressure gradient, just downstream of it. Differences are seen on the pressure gradient upstream of the shock and also on the Mach number level on the lower side. These differences are attributed to 3D effects due to model chord length (250mm) with respect to the dimensions of the T2 cross-section: 390x400 mm^2. Moreover, these differences exist whatever angle of attack or Reynolds number are considered.

3D results

Thus, 3D computation has been performed in order to be as close as possible to the test conditions. A 3D mesh has been generated with ICEM code and takes into account adaptive upper and lower walls (Fig. 2). The (X,Z) plane contains five domains (33289 grid points). According to 2D results, the mesh is refined in the shock region. The upstream section location of the mesh has been adapted to guess the correct boundary layer thickness on the upper and lower walls at the test section entrance. Due to grid convergence study (Furlano, 2001), the 3D mesh characteristics are: i) a number of 97 identical (X,Z)-planes in the lateral direction (3,494,000 grid points); ii) a height of the first grid point in the direction normal to the side wall less than 2 wall units.

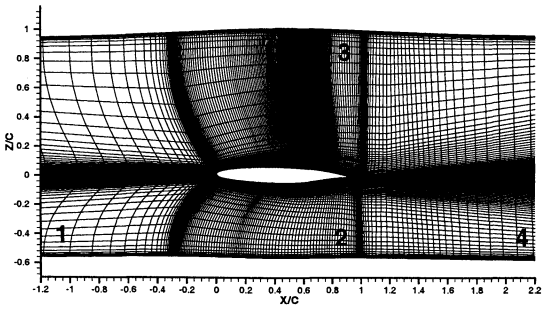

Figure 2: Mesh of the OALT25 airfoil.

The constant pressure in the exit section (X/c=3.75) of the mesh volume has to be adjusted in order to get the right flow rate within the test section: it is equal to about 66% of the free-stream stagnation pressure.

Computations have been carried out without any correction to M_∞ and α, and the [Sm] model has been the only chosen candidate. To reach convergence, about 30000 iterations are necessary, i.e. 130 CPU hours on the NEC SX5 computer.

Pressure distributions at several lateral positions are provided in Figure 3, especially on the last fourth of the airfoil span, close to the side wall; e represents half wing span of the model. Three-dimensionality of the flow is clearly noticeable: the shock wave footprint varies over a bit more than 16% chord length in the free-stream direction, linked to a more or less important extent of the supersonic flow area. When looking at the longitudinal pressure distribution, along the centre-line of the model, 3D computations allow to reach a better agreement on the suction side, on the pressure gradient upstream of the shock and on the shock location (Fig. 3) than 2D ones carried out without any boundary (cf. Fig. 1).

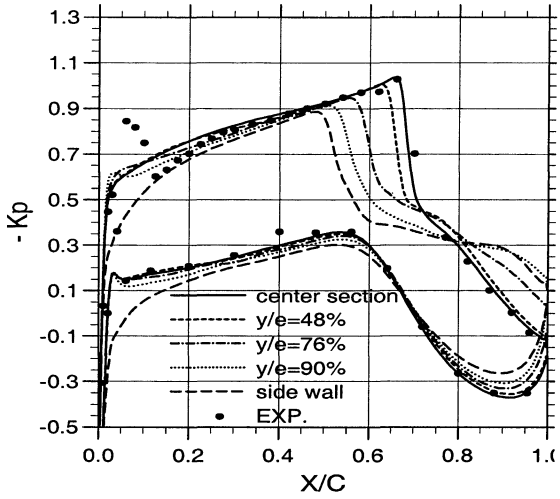

Figure 3: OALT25 airfoil. Pressure distribution. [Sm] model. M_∞=0.78, α=1°, Rc=20.15 10^6.

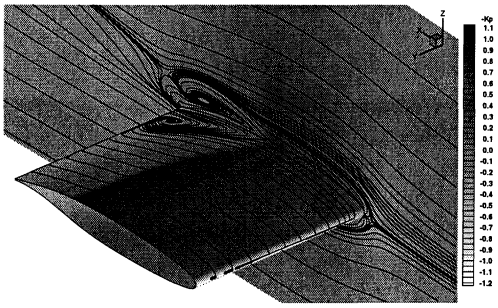

Figure 4: OALT25 airfoil. Contours of –Kp and skin-friction lines pattern. [Sm] model. M_∞=0.78, α=1°, Rc=20.15 10^6.

The contours of the local pressure coefficient are displayed in Figure 4, showing the three-dimensionality of the flow in the area close to the trailing edge and to the side wall. Separation is well evidenced from the friction line pattern; it is also possible to point out the footprint of the horse shoe vortex on the side wall, upstream of the leading edge/wall junction.

Furthermore, the computed pressure distribution along the adaptive upper and lower walls is really good, validating then this approach (Fig. 5). Along these walls, there is not so much 3D effects, except at x/c~1 on the lower side. In this area, first of all the airfoil loading is rather important, and secondly, the airfoil is closer to that wall (Fig. 2).

3D results are in better agreement with experiments than 2D ones when comparing the

location of the shock, the local Mach number upstream of the shock and the pressure level at the trailing edge of the airfoil (Fig. 6). Three-dimensionality of the flow really exists for y/e greater than 30%. At this angle of attack, the flow is not separated in the trailing edge region until y/e=50%; then, between 85% and 100% the effect of the side wall is clearly noticeable on $-Kp_{TE}$.

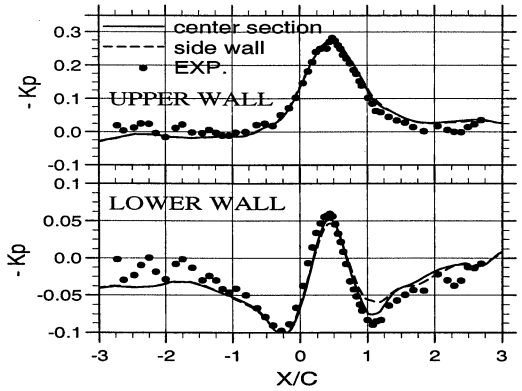

Figure 5: OALT25 airfoil. Pressure distribution on the upper and lower walls of the test section. [Sm] model. M_∞=0.78, α=1°, Rc=20.15 10^6.

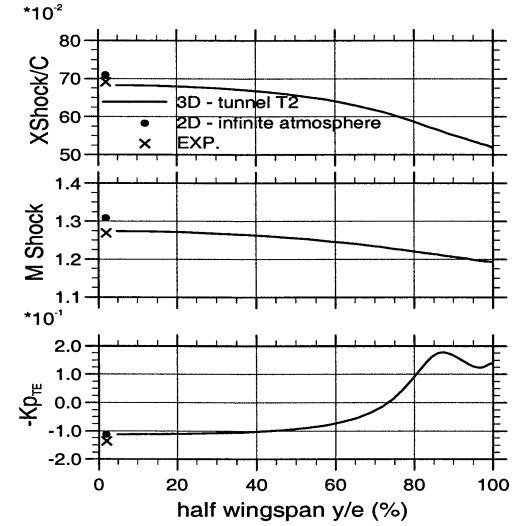

Figure 6: OALT25 airfoil. Lateral evolutions of shock location, local Mach number upstream of the shock and pressure level at the trailing edge.

2D UNSTEADY TRANSONIC STUDY: RA16SC1 AIRFOIL

Experimental test conditions

Tests were conducted in the ONERA S3 wind tunnel with the 2D RA16SC1 airfoil (c: 180mm, e/c=16%), at M_∞=0.732 and Rc=4.2 10^6. Transition was tripped on both sides of the airfoil at x/c=7.5%. Steady pressure field, from 78 pressure taps, is available at α=3°, corresponding to the entrance of buffeting regime. Kulite sensors provide r.m.s values of the pressure at higher values of the angle of attack.

Steady state computations

First of all, steady-state computations have been performed for α=4°. Corrections have been made to take into account the side walls influence (ΔM_∞=-0.009 and $\Delta\alpha$=-1.0°). Steady-state solutions have been obtained with a grid (337*105 points) for which the reduced height y^+ of the cell adjacent to the wall is about 1.5-1.8. For meshes with smaller reduced height, convergence has never been reached whatever turbulence model ([Sm], [JL], [SA] or [KPHI]) is considered. These convergence problems may be partially attributed to local time stepping.

This steady-state flow field has been used as initial solutions for the unsteady runs.

Unsteady results

Applying 2D unsteady RANS computations allows to reach well-established oscillations on the lift coefficient (Fig. 7). It could be noticed that the mean average of these oscillations does not correspond to the steady value.

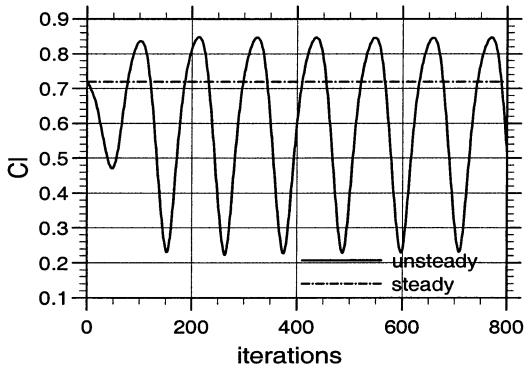

Figure 7: RA16SC1 airfoil. Evolution of the lift coefficient versus time. [Sm] model. M_∞=0.732, α=4°, Rc=4.2 10^6.

Pressure distributions for several time intervals within a time period are given in Figure 8; the shock location moves over almost 30% chord length according to the zero-pressure gradient upstream of the shock. The importance of the plateau close to the trailing edge points out the extent of the separation region.

During an oscillating period of the shock, four phases can be clearly identified:

- Phase A: shedding of the vortex structure due to large separation area between the shock wave position and the trailing edge, shock weakening and slow downwards motion;
- Phase B: important downwards motion of the shock wave (25-30% chord length) without any separation on the rear part of the airfoil;
- Phase C: greater shock wave strength, with separation first due to the shock/boundary layer interaction, then in the trailing edge vicinity;
- Phase D: upwards motion of the shock without any increased intensity, connected to strong separated region.

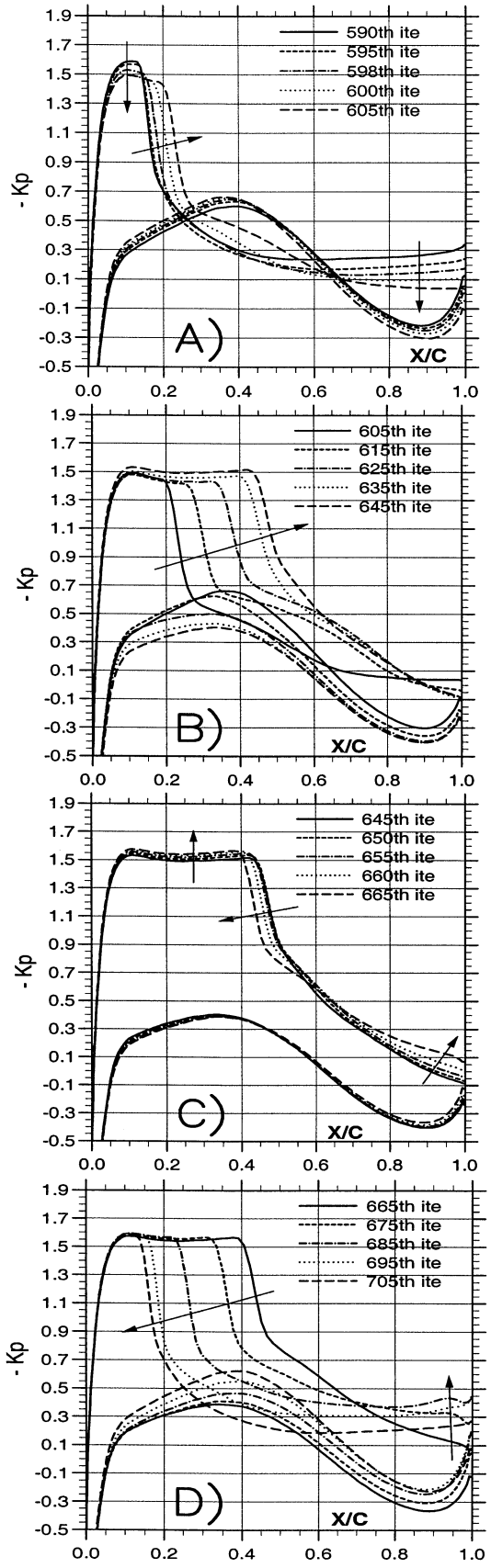

Figure 8: RA16SC1 airfoil. Evolution of the pressure distribution versus time. [Sm] model. M_∞=0.732, α=4°, Rc=4.2 10^6.

Instability of the separation at the shock wave foot appears to be the starting point of the buffeting process. The sudden escape of vorticity, associated with strong re-circulating flows and shock displacement, provokes self-sustaining oscillating flow (Furlano, 2001).

The computed level of the root mean square value of the pressure fluctuations is in rather good agreement with the measured one, on the pressure as well as suction sides (Fig. 9). The resulting computed frequency of the turbulent motion is smaller than the measured one: 86 Hz vs. 100 Hz.

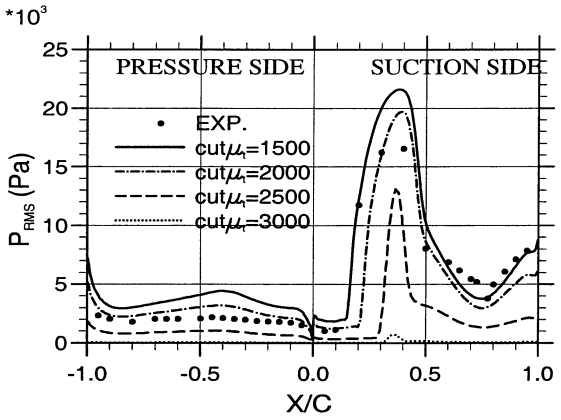

Figure 9: RA16SC1 airfoil. Distribution of the r.m.s value of the pressure. [Sm] model. M_∞=0.732, α=4°, Rc=4.2 10^6.

Figure 9 points out the determinant effect upon unsteadiness of the threshold level ("$cut\mu_t$") of the maximum value of the turbulent viscosity. Physical flow oscillations are provided with rather low value of this parameter (the above-analysed results correspond to $cut\mu_t$=1500). The action of this parameter is to restrict the maximum turbulence level in areas of massive re-circulating flows. Such a dependency cannot be hidden; a possible explanation could be attributed either to a coarse grid mesh close to the airfoil, or to the turbulence model ([Sm]) that has been chosen.

Regarding the former point, non-dependency of flow oscillations to $cut\mu_t$ by using a finer mesh and [JL] turbulence model have been recently obtained by Rouzaud.

Therefore, recent calculations carried out on that same airfoil test case, but using another approach - two-layer closure with wall functions in the inner layer and transport equation models in the outer one, (Goncalves and Houdeville, 2001) - have pointed out that flow oscillations could be obtained by using [JL] or [SST] turbulence models, while damping was provided using [Sm] model.

Work is under progress in these two directions, by testing other turbulence models and using refined mesh size, in order to try to get rid of such parameter influence.

CONCLUSIONS

Results presented in this paper are devoted to computations of turbulent flows that develop on airfoil, at conditions close to airfoil buffeting. Using the ONERA RANS solver and turbulence closure provided by transport equation models, steady computations have been performed with the objective of turbulence validation. In that case, models such as Spalart-Allmaras, k-l Smith, k-ω/k-ε Menter with SST corrector-type or k-l/k-φ from ONERA provided rather satisfactory results. Nevertheless, such computations have pointed out the limitation of the 2D steady approach.

Thus, 3D computations made for the OALT25 airfoil, by considering the exact testing conditions, have revealed the necessity to perform such an exercise. Such runs are very sensitive to mesh grid refinement, especially in the vicinity of the side wall, and to initial conditions at the entrance test section, yet. Nevertheless, 3D effects play undoubtedly an important role for predicting buffet onset of a 2D airfoil imbedded in the side walls of a tunnel test section. These computations were made with the k-l turbulence model; the use of another turbulence model should not modify the main conclusions of that study.

Furthermore, the first unsteady computations, carried out with the RA16SC1 airfoil, are very encouraging. They have allowed to suggest a scenario regarding 2D buffeting aspects, with the different associated phases. These calculations have shown the influence of a given parameter on the numerical results; indeed, a cut-off value on the eddy viscosity affects tremendously the shock oscillations. Such a limitation is under detailed scrutinization at ONERA, since it could be attributed to either the mesh size or the turbulence model. The point that can be questionable is to wonder whether unsteady computations can be run up with turbulence models schemes expressed as for steady ones.

Acknowledgements

The authors gratefully acknowledge the Service des Programmes Aéronautiques which granted the research reported in this paper.

The authors wish to express their gratitude to Dr. B. Aupoix for providing useful comments to enhance the final version of the paper. At last, the two first authors are grateful to C. Gleyzes for providing meshes and to E. Goncalves & R. Houdeville for fruitful discussions.

References

Caruana D., Mignosi A. and Bulgubure C., 1996, "Experimental study on Transonic Shock wave turbulent boundary layer interactions and separation instabilities", in Proc. ICAS Sorente 9-10 Sept., ICAS-96-2.1.3.

Couaillier V., 1999, "Numerical simulation of separated turbulent flows based on the solution of RANS/Low Reynolds two-equation model, AIAA Paper 99-0154.

Cousteix J., Saint-Martin V., Messing B., Bézard~H. and Aupoix B., 1997, "Developments of the k-φ turbulence model", in Proceedings 11th Symp. on Turbulent Shear Flows, Grenoble, September 8-11.

Furlano F., 2001, "Comportement de modèles de turbulence pour les écoulements décollés en entrée de tremblement", Ph.D. Thesis, ENSAE, 14 Mars.

Furlano F. and Coustols E., 1999, "Validation de modèles de turbulence pour les écoulements décollés proches du tremblement", 14ème Congrès Français de Mécanique, Toulouse, 1–3 septembre.

Goncalves E. and Houdeville R., 2001, "Re-assessment of the wall functions approach for RANS computations", Aerosp. Sci. Technol., Vol. 5, pp. 1-14.

Jameson A., 1991, "Time dependent calculations using multigrid, with applications to unsteady flows past airfoils and wings", AIAA Paper 91-1596.

Jameson A., Schmidt W. and Turkel E., 1981, "Numerical solution of the Euler equations by finite volume methods using Runge-Kutta time stepping schemes", AIAA Paper 81-1259.

Jones W.P. and Launder B.E., 1972, "The prediction of laminarization with a two-equation model of turbulence", Int. J. of Heat and Mass Transfer, Vol. 15, No. 2, pp. 301-314.

Menter F.R., 1994, "Two-equation eddy-viscosity turbulence models for engineering applications", AIAA Journal, Vol. 32, No. 8, pp. 1598-1605.

Rouzaud O. and Plot S, 2000a, "Numerical simulation of unsteady internal flows using dual time stepping method", 1st International Conference on CFD, Kyoto (Japan).

Rouzaud O., Plot S. and Couaillier V., 2000b, "Numerical simulation of buffeting over airfoil using dual-time stepping method", in Proc. ECCOMAS 2000, Barcelone, 11-14 September.

Smith B.R., 1994, "A near wall model for the k-l two-equation turbulence model", AIAA Paper 94-2386.

Spalart P.R. and Allmaras, 1994, "A one-equation turbulence model for aerodynamic flows", La Recherche Aerospatiale, Vol. 1, 5-21.

Thomas J.L. and Salas M.D., 1986, "Far-field boundary conditions for transonic lifting solutions to the Euler equations", AIAA Journal, Vol. 24, No. 7, pp. 1074-1080.

Vuillot A.M., Couaillier V. and Liamis N., 1993, "3D turbomachinery Euler and Navier-Stokes calculation with a multi-domain cell-centered approach", AIAA Paper 93-2576.